Vibrations and cultural heritage preservation: a new approach to protect objects

Forma Loïc, Boutin Henri, Jossic Marguerite, Le Conte Sandie, Wilkie-Chancellier Nicolas

Vibrations and cultural heritage preservation: a new approach to protect objects.

Forma Loïc[1,4,5*], Boutin Henri[1], Jossic Marguerite[2,3], Le Conte Sandie[4] and Wilkie-Chancellier Nicolas[5]

[1]Sciences et technologies de la musique et du son , Ircam, 1 place Igor Stravinsky, Paris, 75004, France.
[2]Equipe Conservation recherche, Musée de la Musique, Cité de la musique / Philharmonie de Paris, 221 avenue Jean Jaurès, Paris, 75019, France.
[3]Centre de recherche sur la conservation, Muséum national d'histoire natuerlle / Ministère de la culture, 36 rue Geoffroy Saint-Hilaire, Paris, 75005, France.
[4]Laboratoire de Recherche, Institut National du Patrimoine, 124 rue Henri-Barbusse, Aubervilliers, 93300, France.
[5]Laboratoire Systèmes et Applications des Technologies de l'Information et de l'Energie SATIE, CY Cergy Paris Université, 5 mail Gay Lussac, Neuville, 95000, France.

*Corresponding author(s). E-mail(s): loic.forma@ircam.fr;

Abstract

Vibrations of cultural objects due to different sources (transport, exhibitions, local works) have recently been raising more and more interest from the heritage community. Consequently, the development of anti-vibration protection systems has become a major issue. However, most of the proposed solutions suffer from a lack of adaptability, practicality and effectiveness. To overcome these limits, this paper investigates the possibility to design a vibration control system based on the active control technique, whose purpose is to cancel out the disturbance vibration by creating an opposite vibration. This approach, which allows to control vibrations without contact to the object, is particularly suitable for heritage objects protected by cultural ethics rules. To test the feasibility of this approach, an experimental demonstration bench including a reproduction of a museum shelf and

an active control device, composed of sensors and an electrodynamic actuator, is developed. Vibration source signals similar to those previously measured *in situ* are applied to the shelf by a vibration exciter. A classic control algorithm, the Filtered Least Mean Square, is used to control the shelf vibrations. Results point out that the control device is able to reduce the amplitude of harmonic, respectively broadband, primary sources by 37.4 dB in 0.15 seconds and by 14.0 dB in 0.67 seconds. Furthermore, the system is robust to both amplitude and frequency content changes. Finally, a parametric study shows that the greatest vibration attenuation and the fastest control cannot be achieved simultaneously, so the algorithm parameters must result from a compromise.

1 Introduction

1.1 Vibrations of cultural heritage objects

Over the last decades, the cultural heritage community has gradually become aware of the need to protect heritage objects from vibrations, which can represent a potential threat for different reasons. In case of light objects, the energy of vibrations can be high enough to make them move on their stand, with the risk of striking other artefacts or even falling out of the stand. Hopefully, the object's movement is usually slow and museum staffs notice the displacement before a dramatic event happens. However, a less obvious consequence of vibrations is to apply stresses, which in turn induce strain and might initiate the propagation of cracks in the material [1].

Sources of vibrations faced in a cultural heritage context are numerous and multifaceted. Vibrations generated by trucks, planes or trains when objects are transported have been receiving a lot of consideration since the early 90's [2–6]. When objects are exposed or stored in museums, most common sources of vibrations are created by public constructions [7–12] and public transports nearby [13–17]. In some conditions, concerts nearby museums [18, 19], auxiliary devices such as fans and air conditioning units [16] and visitors' footsteps [20] can also be harmful for the objects. Vibrations during objects transportation have been reported to be between 10 and 100 Hz [2–5], while vibrations measured in museums range from 10 to 200 Hz [10, 11, 16, 18, 19, 21–23]

1.2 Protection systems for artworks: an overview

Over the last thirty years, different solutions to protect cultural objects from vibrations have been developed. To ensure objects safety during road transportation, wooden boxes filled with cushion materials such as foams are traditionally used. Most of the time, the size of the boxes as well as the material and its dimensions are chosen based on the experience of the manufacturer. However, these protective systems can be counterproductive if not designed

carefully [4, 5]. In order to make consistent and effective protective boxes, an empirical approach based on measurements during transportation has been proposed in previous works [2, 3, 5]. The effectiveness of this strategy, although proven by the results, depends on many factors such as the position of the box inside the truck. To overcome these limits, an integrated approach including complete 3D scan of the object, finite element analysis and rapid prototyping has been proposed [6] to build customed packages, which take into account both the artefact geometry and its points of fragility.

Most of the cultural objects exposed or stored in museums are either suspended from or laid on a base. In the case of paintings, several studies investigate the use of backing boards as anti-vibrations protective systems [4, 24, 25]. Their performance ranges from highly effective to counterproductive, depending on many parameters (board material, distance between the board and the painting...). In addition, numerical simulations hardly predict the experimental behaviour. Genevaux [26] introduced a procedure for designing anti-vibratory systems for stretched paintings with a flexible mounting placed between the wall and the canvas. An equivalent system has then been proposed by Higgit [10], with dampers made of viscoelastic elements added to the hangers of paintings. Although these systems reach their anti-vibration objectives, they require a preliminary study to adapt to the physical characteristics of the paintings. Regarding objects laying on a base, isolating elements such as foams, springs or anti-vibratory rubbers placed between the floor and the base have been extensively studied to mitigate vibrations [7, 8, 15]. Some works also propose to experimentally study the floor behaviour [16], in order to place the object where the vibration level is minimum. Finally, magnetic levitation systems can be used to mitigate vertical vibrations of light statues [27].

When it is not possible to directly protect an artefact with usual systems, or when vibrations impact the whole building, one often chooses to protect structural elements of the building instead of designing protection systems on a case-by-case basis. For instance, tuned mass dampers can be fixed to the floor in order to absorb and dissipate energy [8]. Higher performances can be reached by attenuating the propagation of solid waves through public works solutions: for instance, it is possible to increase the floor stiffness by adding columns supported on spread footings below the basement slab [20]. To reduce vibrations transmitted by underground railway tracks at Musée d'Orsay (Paris, France), a study [14] was conducted to choose the most effective track coating. At Villa Farnesina (Rome, Italia), a structural restoration of the floor has been performed by adding a thick concrete base with added damping properties [17]. A noticeable case has also been provided by the Museum of the Viking Age (Oslo, Norway), which decided to build concrete screen walls in the ground to reflect vibrations created by a construction site nearby [12]. Furthermore, the case of construction works is somehow special because it offers museums the opportunity to anticipate a solution. Thus, a methodology called "Integral Approach", which emphasizes the importance of constant vibrations

monitoring and good communication with construction supervisors, has been developed and improved over years [7–11, 21].

1.3 Active control basics

All the solutions described in the previous section are based on passive control strategies: they use the physical properties of materials, such as damping, mass and stiffness, to mitigate vibrations. In the literature, passive solutions are often distinguished from active control strategies [28, 29] which mitigate vibrations by means of electronic components which bring energy.

The principle of active control is to cancel out the vibrations suffered by an object and generated by a disturbance source, with the help of an electronic secondary source (actuator or loudspeaker), which sends the opposite vibration to the object (Figure 1). In practice, one of the main challenges of active control is to determine the command to send to the actuator. The effectiveness of the control relies on an algorithm capable of calculating the appropriate control signal and a digital processor capable of providing this control to the actuator with minimum latency. The control performances are assessed with one error sensor or more, measuring the residual vibration. Active control has historically been designed as a strategy for reducing sound levels, with the first patent [30] and first application [31] describing it as an electronic sound absorber. It has also been successfully applied to vibrating structures, as in the domain of automotive [32, 33], aeronautic [34, 35] and construction with anti-seismic buildings [36]. In the domain of cultural heritage, the use of an anti-seismic active control system has been theoretically studied in [37], but no experimental demonstration has been implemented so far.

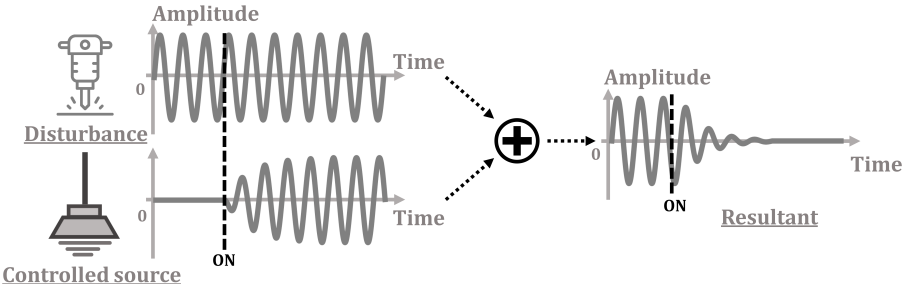

Fig. 1 Physical principle of active control. The vibration created by the disturbance source (top left) is cancelled thanks to a controlled source producing an opposite vibration (bottom left). Thus, the sum of the two vibrations is zero (right). This drawing emphazises the moment when the control is activated, at time equal to "ON".

1.4 Objectives of the study

Most solutions addressing the problem of vibrations attenuation (cf 1.2), although often effective, are constrained by the necessity of preliminary studies

or construction works, their limited range of applications, or their non-reusability. As an attempt to address these limitations, this study proposes to develop an anti-vibration device adapted to a large-scale use in a cultural heritage context. This paper focuses on the development and the technical validation of an active vibration control strategy, and a proof-of-concept. The main objective is to demonstrate that active control can be used to protect cultural heritage objects. The search for an optimal solution is out of the scope and will be addressed in future works.

To overcome the limits of the anti-vibratory solutions previously mentioned, a set of specifications has been developed to meet the needs expressed by professionals in cultural heritage institutions. In order to respect cultural ethics, the system must be non-intrusive, reversible, and as discrete as possible so as not to interfere with the museography. Four main requests are expressed by cultural actors: (i) the device must be effective to mitigate vibrations created by sources commonly found in cultural heritage context, i.e. be performant in a carefully chosen frequency range (ii) the device must be adapted to the large diversity of objects no matter their display systems (iii) the device must be easy and fast to install or remove (vi) the device must be able to stay effective when environmental conditions (such as vibrations sources) change.

The active control solution described in this article aims to minimise the vibrations of cultural heritage objects, while respecting these demands. First, the motivations and the active control strategy are detailed with an overview of the control algorithm. Then, the protocol used to apply the control solution to an experimental museum shelf mock-up is described. The device performances will be measured using two indicators: one quantifies the reduction in vibration energy, the other estimates the speed of control convergence. Results obtained with different realistic disturbance signals are introduced, and the influence of some control parameters on the indicators of performance is investigated. Finally, perspectives to improve the system performances are discussed.

2 Methods

2.1 Active control solution

When choosing the control strategy, two key points must be addressed: the capacity of the strategy to mitigate vibrations, and the possibility to adapt this strategy in real life, from practical perspectives. Usually a trade-off between effectiveness and practicality is needed.

The choice of a control strategy is strongly influenced by the frequency range of the vibration sources. In a cultural heritage context, analyses from signals recorded in museums pointed out that the vibration energy is mostly concentrated in the lower frequency range, from about ten to a few hundred hertz [8, 22, 38]. These results were confirmed by several measurements performed in the project's partner museums. An example is shown in Figure 2. Two accelerometers were fixed with wax on two shelves supporting aboriginal

Oceania artefacts at Musée du Quai Branly (Paris, France). The acceleration of the shelves was recorded (i) in the absence of vibrations sources – other that the ambient noise in the exhibition room – and (ii) in the presence of the noise created by the sliding door of the showcase where the objects were exposed. Results show that the vibrations of the sliding door induce vibrations to the shelves between 10 and 400 Hz (Figure 2). These results are consistent with the frequency range commonly expressed in the literature (10-200 Hz). According to these measurements, the target frequency range for the development of the active control solution is [10 Hz - 400 Hz].

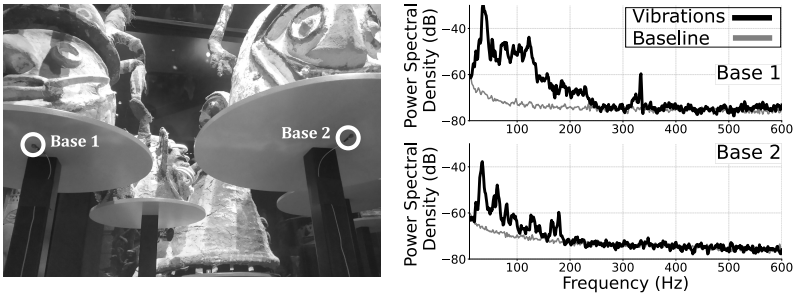

Fig. 2 Left: picture of two artefacts with their base equipped with an accelerometer at Musée du Quai Branly, Jacques Chirac (Paris, France). The accelerometers positions are indicated by two white circles. Right: power spectral density of signals measured by accelerometers. In the absence of vibrations (solid grey line) and in the presence of vibrations due to the showcase sliding door (solid black line).

Passive solutions are not effective to control these low frequency vibrations in a cultural heritage context for at least two reasons: (i) the lowest the frequency range to be attenuated, the largest and heaviest the protective device must be, which is not convenient for most applications in a cultural heritage context [31] (ii) passive systems have no adaptation capacity, thus efficient systems can become counter-productive if the source characteristics change [4, 5]. Alternatively, the principle of active systems is particularly relevant to cancel low frequency vibrations. Also, active systems are composed of transducers which are easy to install and remove on a wide variety of shapes and materials. Finally, a strong benefit of active control is the opportunity to use adaptive algorithms, that update in real time and remain effective when environmental conditions change. Therefore, active control appears to be a good match between effectiveness and practicality.

In museums, most of the vibrations transmitted to an object must pass through its holder. As a consequence, the present project aims at developing a control system to minimise the vibrations of the supports on which the objects are exposed or stored. Such an approach ensures the integrity of the objects, as the control device is not in contact with them.

2.2 Feedforward control

2.2.1 General Presentation

In the following, all scalar physical quantities are shown in italic, and vector quantities are shown in bold. A feedforward control system, depicted in Figure 3, is composed of two accelerometers, respectively called reference and error, an actuator, called secondary source, and a controller represented by the control filter block. The purpose of the control device is to cancel out the vibration created by the source of disturbance, called primary source, at the position of the error accelerometers, by the means of the secondary source which aims to create an opposite vibration, as explained Figure 1. The contribution from the primary source is noted $p(t)$ at the reference sensor and $d(t)$ at the error sensor. To cancel the vibration $e(t)$ measured by the error sensor, the controller sends a command $u(t)$ to the actuator in such a way that the contribution $y(t)$ of the actuator at the error sensor is the opposite of the perturbation $d(t)$. The error accelerometer provides an indication of the effectiveness of the control system by measuring the residual vibration $e(t)$, while the controller aims to minimise this error signal. The reference accelerometer $x(t)$ is used to capture the disturbance vibration $p(t)$ before it reaches the object. However, measurement of $x(t)$ is biased by the contribution $r(t)$ of the secondary source at the reference. This control configuration is named "feedforward" as it uses both a reference sensor and an error sensor, and feeds the controller with the reference signal. In this case, the error signal is used to update the control filter parameters. In contrast, the "feedback" configuration [29] requires only one error sensor and feeds the error waveform to the controller.

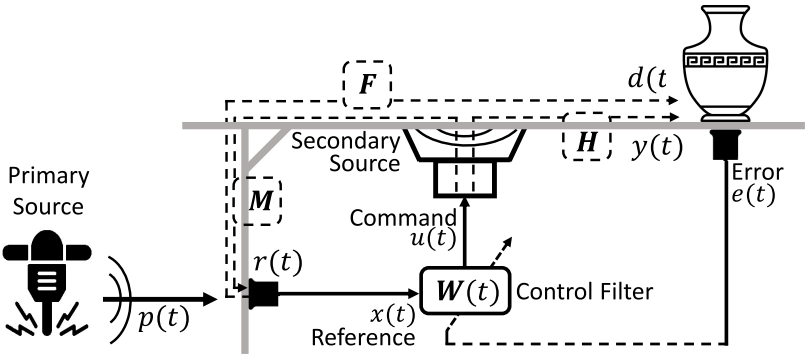

Fig. 3 Schematic overview of the feedforward control solution used in the present work. The control system is composed of two accelerometers (Error and Reference), an actuator (secondary source) and a controller (control filter). **F**, **H** and **M** represents respectively the primary, secondary and reverse path. Noise measurements have been neglected, while **F**, **H** and **M** are assumed to be time invariant.

It is possible to define the primary path **F** as the transfer function between $p(t)$ and $d(t)$, which is a mathematical function describing the signal modifications when going through the physical path between the reference and

the error. The secondary path $\mathbf{H}$ is the transfer function between $u(t)$ and $y(t)$, which describes the signal modifications when going through the electronic and physical paths between the actuator input and the error sensor output. Similarly, the reverse path $\mathbf{M}$ is the transfer function between $u(t)$ and $r(t)$, which describes the signal modifications when going through the electronic and physical paths between the actuator input and the reference sensor output. Finally, the command sent to the secondary source is computed by filtering the reference $x(t)$ by a so-called control filter whose vector of coefficients is denoted $\mathbf{W}(t)$. In this paper, the control strategy is said to be adaptive, because it uses the error signal to update the coefficients of $\mathbf{W}(t)$ over time. This allows the controller to adjust its behaviour when the primary source of vibration changes.

2.2.2 Control Configuration of the study

Figure 3 not only depicts a feedforward control configuration, but also emphasises on how an active control strategy can be set to protect cultural objects. As stated previously, the transducers cannot be in direct contact with objects due to cultural ethic rules. Thus, the chosen solution consists into equipping the object stand with the error accelerometers placed as close as possible to the object, to prevent stand vibrations at the object position. Assuming constant contact between the stand and the object, if the stand does not vibrate at the object position, the object does not vibrate either. Finally, the reference sensor, whose purpose is to capture a measurement of the perturbation before it reaches the object, is placed at the stand base, while the secondary source is placed between the two accelerometers. In practice, it is convenient to place it as far as possible from the reference in order to reduce the bias of the reference measurement, i.e. to minimise the contribution of the reverse path $\mathbf{M}$.

To sum up, the controlled system is composed of both the object and its support, and the aim of the control is to minimise the support vibration at the object position (where the error sensor is placed).

It should be noted that the vibration measurements are corrupted by many undesirable biases that have been neglected in Fig. 3 for the sake of readability: background vibrations, background electronic noise, electromagnetic perturbations, unperfect analog to digital converters.... However, in the current situation, vibration levels are assumed to be high enough to neglect these external perturbations. In addition, external factors such as temperature and humidity are likely to modify the mechanical properties of the stand with time and consequently the transfer functions. In the context of a museum where these factors are drastically controlled, one can assume that transfer functions shown in Fig. 3 do not depend on time.

2.3 Control Algorithm

2.3.1 Feedforward adaptive Algorithms

As stated in the objectives, the purpose of the paper is to provide a feasibility study and no to seek for an optimal control solution. This is the reason why we choose to use the Filtered Least Means Square (FxLMS) algorithm [28], a proven algorithm that is fast to implement, fairly robust and therefore still widely used. Many current algorithms outperform FxLMS performances and future works will focus on improving performances of the control device. This section introduces some of them.

The FxLMS algorithm searches for the finite impulse response (FIR) control filter $\mathbf{W}(t)$ that minimises the mean square error, by updating the coefficients of $\mathbf{W}(t)$ with a steepest descent procedure. As FIR filters require many coefficients to reach good performances, similar algorithms have been designed to work with infinite impulse responses control filters to reduce algorithm numerical complexity [39]. However, these algorithms do not account for the reverse path $\mathbf{M}$, which can lead to strong stability problems.

In order to take the reverse path into consideration, other algorithms remove from the reference an estimate of the secondary source contribution [40]. However, this technique called "Feedback Neutralization" is very sensitive to the quality of the transfer function estimation and results in very unstable systems [41]. An improved version updates in real time the estimation of the reverse path to ensure stronger stability, but it requires to add noise to the control signal, what decreases control performances [42]. An approach based on the ordinary differential equations method of Ljung [43], has been proposed [44] to develop and ensure the stability of adaptive algorithms in the presence of a reverse path. However, strong assumptions such as vanishing adaptation gain are made and the stability of the algorithm is no more guarantee if a non-vanishing gain is used to keep adaptation capabilities [45].

One of the most promising approaches consists in using the Youla-Kuçera parametrization, which simultaneously guarantees the stability of the internal loop and update the controller [45]. Many algorithms based on the Youla-Kucera parametrization have been developed, and experimental results show that even simple form of this parametrization can reach satisfying performances [46].

2.3.2 Filtered Least Mean Square Algorithm

The block diagram in Figure 4 shows a general view of an active feedforward control solution. $\mathbf{F}$ and $\mathbf{H}$ represents respectively the primary and secondary path, as depicted in Figure 3, while $\hat{\mathbf{H}}$ is a numerical estimation of the secondary path. The control filter $\mathbf{W}(t)$ is updated using an LMS procedure described in the next paragraph. Note that the reverse path is ignored because the FxLMS algorithm neglects the contribution of the secondary source in the reference signal. Consequences of this assumption will be discussed later (see Section 5).

The coefficients of the control filter $\mathbf{W}(t)$ are updated at every time sample in order to minimise the error energy $e^2(t)$. To do that, the so-called Least Mean Square block (LMS in Figure 4) uses the gradient descent algorithm, which updates the filter coefficients using a recursive equation of the form $\mathbf{W}(t+1) = \mathbf{W}(t) + \alpha \times f(e(t+1), x(t+1))$. α is an adaptation gain set by the operator and f is the correction function $f = e(t+1)\mathbf{H}x(t+1)$. At every time sample, the controller coefficients are thus updated, by adding a correction term which is a function of the measured signals. Actually, the correction function given just above is purely theoretical, as in practice it is not possible to perfectly know the transfer function of the secondary path. However, it is possible to get an estimation $\hat{\mathbf{H}}$ of this transfer function, and the correction function used in practice is $f = e(t+1)\hat{\mathbf{H}}x(t+1)$

In this work, the normalised version of the FxLMS is preferred for stability and robustness reasons. This version updates the filter coefficients using the same equation as the FxLMS algorithm but normalises the reference signal, so that the adaptation time (see section 3.3) does not depend on the level of the reference anymore. The reader seeking for more information about the FxLMS algorithm and its normalised version can refer to [28, 47]. The block diagram of this algorithm, displayed in Figure 4, describes the procedure to update the controller coefficients.

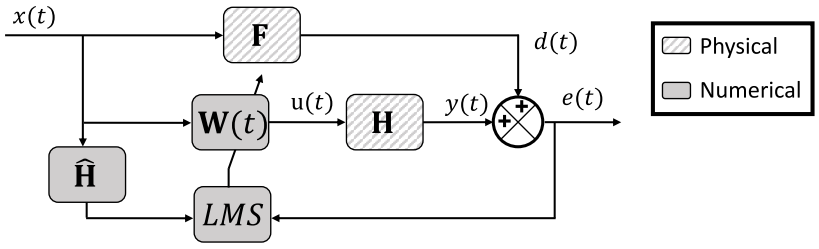

Fig. 4 Block diagram of the controlled system with a FxLMS control algorithm. The primary, and secondary path are respectively represented by the transfer functions $\mathbf{F}$ and $\mathbf{H}$, while $\hat{\mathbf{H}}$ is an estimation of the secondary path. $x(t)$ and $e(t)$ represent respectively the measurements of the reference and error sensors. The controller $\mathbf{W}(t)$ is continuously updated by the mean of a LMS procedure using the error as input. The reverse path has been neglected.

The FxLMS algorithm relies on several inputs that the user must specify:

- An identification procedure aimed to provide an estimate of the secondary path, designed by $\hat{\mathbf{H}}$, used in the FxLMS equations;
- The order of the control filter: a finite impulse response filter is used, whose length denoted Length($\mathbf{W}$) in the following is determined by the operator;
- The adaptation gain α, dedicated to minimise the duration of the adaptation process.

The procedure of the FxLMS algorithm is summarised in three steps, repeated at every time sample:

1. At time t, the controller sends the command $u(t)$, while the reference $x(t)$ and error $e(t)$ are recorded.
2. The error and the reference filtered by a secondary path estimate $\hat{\mathbf{H}}$ are used to compute the new control filter coefficients by means of a Least Mean Square (LMS) procedure.
3. The controller computes the command to be sent at time $t+1$, by filtering the reference with the new control filter.

3 Experiment

3.1 Test Bench

3.1.1 Choice of the actuator

Active control systems create the opposite vibration thanks to a transducer, an electronic device able to convert electric signals into vibrations. One of the main limitation of transducers is their capacity to only operate in a reduced bandwidth, their lower frequency limit being related to their size: the bigger the transducer, the lower the cut-off frequency. In museums, many sources create vibrations with frequency range below 100Hz, such as metro [15], air conditioning systems [15] and can reach a few tens of Hertz in case of visitors [22]. To reach such low frequencies, the actuator must be relatively large - but still much smaller than passive systems that are visually invading with the museography. Actually, this drawback must be taken very seriously, because if museums find the system too cumbersome it will not be used. Here, an actuator with a 60Hz cut-off frequency has been judged as a good trade-off between size (53 mm diameter) and performance in low frequencies, but bigger actuator can be chosen if effectiveness of the system in the low frequency region must be privileged.

3.1.2 Presentation

To test the performance of the control algorithm, a test bench composed of three distinct parts is set up (Figure 5). The first part is the structure to control. In this experiment, a shelf used to expose objects at Musée de la Musique (Paris, France) is selected because it is a common display setting. This shelf is made out of aluminium poles screwed together with a Dibond® plate clamped to the shelf brackets, and fixed to an anti-vibration table. The dimensions of the plates are 80 cm × 12 cm × 8 mm.

The second part of the test bench is the excitation system, which aims at reproducing vibrations sources encountered in a cultural heritage context. It is composed of a vibration exciter (Brüel & Kjær, type 4809), linked to the horizontal pole at the base of the shelf with a threaded steel rod, and driven by a signal generator (dSpace, MicrolabBox), which offers the opportunity to play pre-recorded signals.

Finally, the last part of the system is the active control device itself. It is composed of a controller (dSpace, MicrolabBox), two accelerometers (Brüel &

Kjær, type 4374) with their charge conditioning amplifier (Brüel & Kjær, type 2635), and an audio actuator (PUI Audio, ASX05404-HD-R). The MicrolabBox version is DS 1202, the code is generated from the Simulink interface of Matlab R2016B, and the control software is ControlDesk 6.1. The reference and the error accelerometers are fixed to the left end of the horizontal base pole and to the upper left corner of the plate. The actuator is colocalized with the error sensor, as this configuration offers optimized control performances [29]. Precise positions and shelf dimensions are shown in Figure 6.

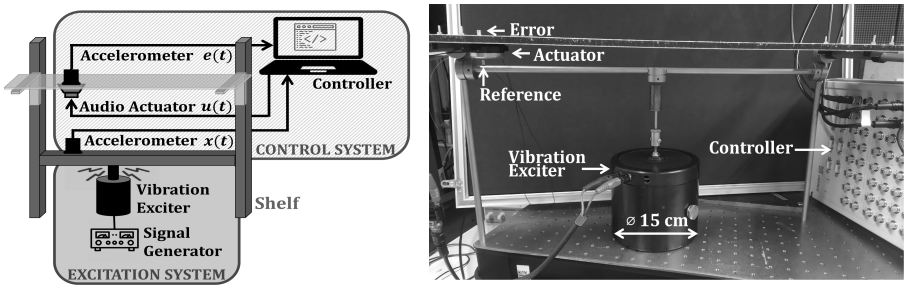

Fig. 5 Drawing (left) and photo (right) of the test bench used during experiments

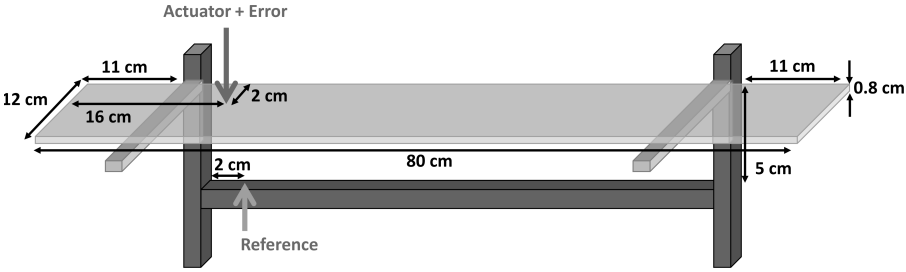

Fig. 6 Drawing of the shelf with dimensions and position of the transducers. Not to Scale.

3.2 Protocol

3.2.1 Secondary path identification

A preliminary stage, without controller, consists in estimating the secondary path $\hat{\mathbf{H}}$. Here, it has been decided to identify this operator in the form of a recursive filter following the four steps procedure described in [48]. First, a command signal is sent to the actuator while the error accelerometer signal is recorded, to get an input-output data set of the secondary path. Second, the number of coefficients to be assigned to the recursive filter, usually chosen with an infinite impulse response, is estimated by an instrumental variable algorithm [49]. Then, the filter coefficients are estimated using the Recursive

Least Square identification algorithm [48]. Finally, a procedure ensures the validity of the filter as an estimate of $\mathbf{H}$, by estimating the calculated output dependency to the measurement noise. If the dependency is above a statistic threshold, the number of filter coefficients is increased and the coefficients values are re-estimated until passing the validation test.

A complementary test is to compare the secondary path frequency response with its identification. The frequency response of the secondary path is calculated from the cross power spectral density of the input-output data set, divided by the power spectral density of the input. To get the frequency response of the estimated secondary path, a new output signal is calculated by filtering the input through the estimated filter. The calculation described above is then computed with this new input-output data set.

3.2.2 Control tests

Tests have all been performed with the same controller configuration. Considering the frequency range of vibration sources in cultural heritage context (10-400 Hz), the sampling frequency, typically at least equal to 5 times the maximum frequency of the primary source in control applications, is set at 2500 Hz. Furthermore, due to the cut-off frequency of the chosen actuator, the study will focus on a 70 to 400 Hz frequency band.

The test signals used for the primary sources are designed in order to replicate the vibration signals found in cultural heritage environments, both in terms of frequency range and time variations: many sources in museums might vary in terms of amplitude or frequency content, such as a metro coming closer and then going further away or a fan with a varying operating frequency. Even though the FxLMS controller is designed to adapt to non-stationary noises, fast disturbance variations can decrease the control effectiveness [50]. Four configurations are used for the primary source: (i) a pure tone at 160 Hz, to reproduce situations which can be faced in the context of cyclic sources such as fans and engines; (ii) a pseudo-white noise filtered between 70 and 400 Hz, supposed to simulate real-life sources with a broadband spectrum. As the algorithm must be able to adapt to environmental changes, both effects of spectral and amplitude changes are investigated: a spectral change (iii), where a white noise is alternatively filtered every 10 seconds by a bandpass filter between 100 and 200 Hz, and another one between 200 and 300 Hz; an amplitude change (iv) with a pseudo-white noise filtered between 70 and 400 Hz whose amplitude is divided alternatively by 1 and 6 during 10 seconds. The choice of the control parameters α and Length($\mathbf{W}$) is discussed below.

To perform the tests, one of the four disturbance signals is chosen and sent to the vibration exciter. Before the control is set on, the amplitude of the disturbance is varied until it reaches the target value given Table 1. All these values have been chosen to be of the same order of magnitude as signals measured in real life, in situations where damages have been noticed [38]. Once this step is completed, the controller is disabled during ten seconds to

save the initial error signal amplitude. Then the control algorithm is activated and the recording is pursued for fifty seconds.

Table 1 Amplitude of the error before activating the control algorithm.

Signal	Target Error Amplitude ($m.s^{-2}$)
Sinewave 160 Hz	6
Broadband 70-400 Hz	6
Broadband 70-400 Hz High Amplitudes	6
Broadband 70-400 Hz Low Amplitudes	1
Broadband 100-200 Hz	6
Broadband 200-300 Hz	6

3.3 Temporal and frequential performance indicators

On a time domain basis, a key performance indicator is the global reduction of the error amplitude in terms of energy. Here it is given by $R = 20\log_{10}(RMSe_f/RMSe_l)$ where $RMSe_f$ (respectively $RMSe_l$) is the root mean square of the error signal during the first second of the recording (respectively during the last second of the recording).

Another critical descriptor is the convergence time, subsequently noted τ, which is related to the time required by the controller to optimise the filter. It is typically defined as the time needed to reach 64% [51], 95% or 99% [52] of the final global reduction R described above. This descriptor can be extracted from the analysis of the error envelope, which is here computed from the moving root mean square over 2500 samples, while a 64% decreasing is the threshold retained for the convergence time.

Finally, the frequency contents of the error energy before and after activating the controller are computed using the Welch estimate of the power spectral density, and compared.

3.4 Parametric Study

To find the optimal value of control parameters α and Length($\mathbf{W}$) which can hardly be estimated, a parametric study is required. To begin, a reasonably low number of coefficients, usually around 50, is given to the control filter, with an adaptation gain low enough to avoid stability issues, usually around 10^{-2}. Then the procedure described above is applied and repeated with increasing values of Length($\mathbf{W}$) and α. Finally, the global reduction R and the convergence time τ are extracted from each measurement.

In the present case, only the pseudo-white noise signal filtered between 70 and 400Hz is used as disturbance signal during this study, and tested values set are (experiment is conducted to test all possible $\{\alpha;$ Length($\mathbf{W}$)$\}$ pairs) :

$$\alpha \in \{10^{-1.7};\ 10^{-1.6};\ 10^{-1.5};\ 10^{-1.4};\ 10^{-1.3};\ 10^{-1.2};\ 10^{-1.1};\ 10^{-1}\}$$

$$\text{Length}(\mathbf{W}) \in \{50;\ 100;\ 150;\ 200;\ 250;\ 300\}$$

4 Results

4.1 Secondary path Identification

The identification procedure recommends to look for a secondary path in the form of an infinite response filter with 58 numerator coefficients and 56 denominator coefficients. The graphical comparison of the secondary path with its identification, Figure 7, shows that both frequency responses have the same behaviour above 100 Hz. However, below this threshold the curves start to differ, especially in their phase. Finally, from the amplitude curve, one can notice that the gain drops below 60 Hz, what corresponds to the cutoff frequency of the actuator.

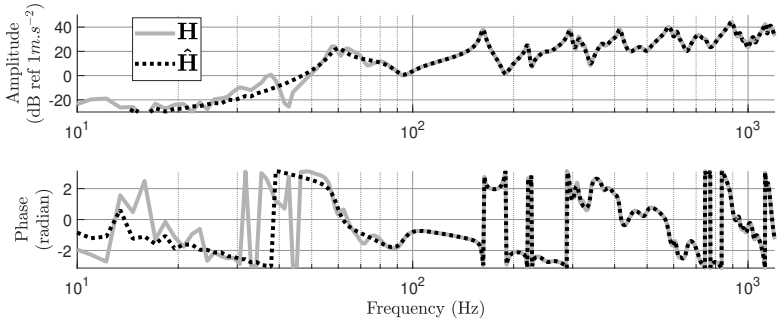

Fig. 7 Frequency response of the secondary path $\mathbf{H}$ and its identification $\hat{\mathbf{H}}$

4.2 Influence of the primary source on control performances

Control results in the case of a single tone excitation of 160 Hz (Figure 8) highlight a strongly effective control system in the time domain, with both a high energy reduction ($R = 37.4$ dB) and a relatively fast convergence ($\tau = 0.15$ s). The main peak of energy is drastically mitigated (by around 60 dB), while other far lower resonances are poorly impacted.

In the case of a broadband disturbance, the algorithm remains effective despite a lower global reduction $R = 13.3$ dB and a slower convergence $\tau = 0.66$ s (Figure 9). The power spectral density analysis underlines the good capacity of the system to control high energy vibrations above 150 Hz; however, the control algorithm fails at controlling vibrations around 100 Hz. Further, the energy is slightly increased below 60 Hz in the control configuration, probably because of the bad phase identification in this frequency range (Figure 9).

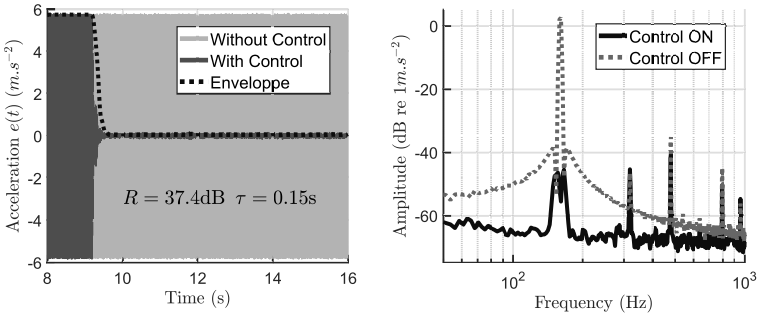

Fig. 8 Control results for a pure tone excitation of 160 Hz. On the left, waveforms of the error with and without control. On the right, power spectral densities of the error signal with and without control. Parameters used for this test are: $\alpha = 10^{-1.5}$, Length($\mathbf{W}$)=150.

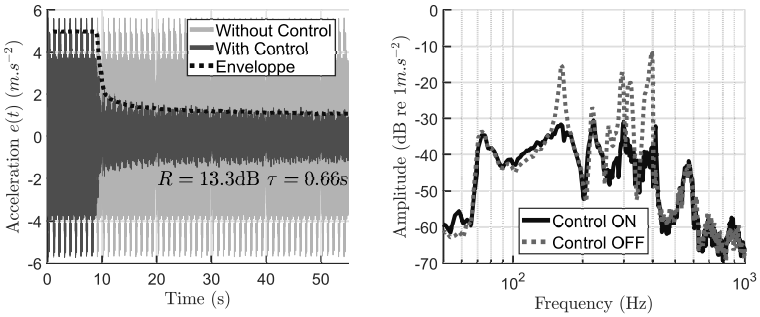

Fig. 9 Control results for a filtered pseudo white noise excitation in the frequency range 70-400 Hz. On the left, waveforms of the error with and without control. On the right, power spectral densities of the error signal with and without control. Parameters used for this test are: $\alpha = 10^{-1.5}$, Length($\mathbf{W}$)=150.

Figures 10 and 11 show the effectiveness of the controller for the configurations (iii) and (iv) respectively, while varying the amplitude and the frequency content of the source. In both cases, variations are chosen as abrupt as possible, i.e. they are instantaneous, to test the algorithm in the worst possible situation. In the first case, the control algorithm is able to significantly decrease the high amplitude vibrations as well as the low amplitude vibrations, with reductions of $R = 12.2$ dB and $R = 11.8$ dB, respectively. While transitions from low to high levels are very smooth and almost instantaneous ($\tau = 0.08s$), the opposite transition is somehow rougher, and the algorithm needs a short time ($\tau = 0.32s$) to recover its optimal behaviour. For the second experiment, it is interesting to note that the control performances are similar for both tested frequency bands of the disturbance: $R = 12.4$ dB for the lower frequency range, $R = 11.1$ dB for the higher frequency range. Furthermore, optimal performances are relatively quickly recovered when the spectral content changes from 100-200 Hz to 200-300 Hz, with a convergence time equal to 0.11 s for transitions from lower to higher range and vice versa.

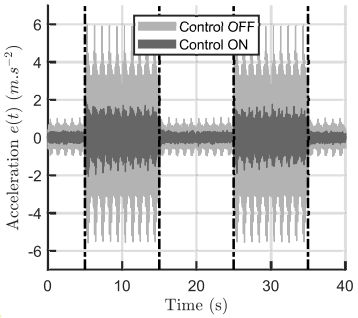

Fig. 10 Control results while varying the amplitude of the primary source. Parameters used for this test are: $\alpha = 10^{-1.5}$, Length($\mathbf{W}$)=150.

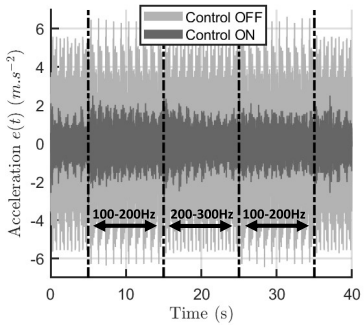

Fig. 11 Control results while varying the frequency content of the primary source. Parameters used for this test are: $\alpha = 10^{-1.5}$, Length($\mathbf{W}$)=150.

4.3 Influence of the algorithm parameters on the control performances

Regarding the effect of the adaptation gain, Figures 12 and 13 present that the adaptation gain is too high to ensure stability of the control loop when it exceeds a limit around $\alpha = 0.1$. In the stability area, the global performances of the algorithm increase with the adaptation gain – higher R and shorter τ– to reach an optimum and finally drop when it gets too close to the limit of stability. Even though the different curves of Figure 12 and those of Figure 11 have the same global shape, their extrema are not reached for the same adaptation gain, and therefore depend on the length of the control filter. Furthermore, the minimum convergence time does not always coincide with the maximum global reduction, particularly when the filter length is equal to 100. As a consequence, a trade-off between the two indicators needs to be done.

While the convergence time is clearly an increasing function of the filter length (Figure 15), the tendency of the global reduction is a little bit more complex, as its rapid increase is gradually slowing down until the curve stabilises and finally decreases slightly (Figure 13). These results underline the impossibility to simultaneously optimise the filter length and the α parameter. Performance measurements on a large number of tests show that the best reduction values are obtained with a filter length greater than a minimum of 100 coefficients. However, increasing the length also reduces the convergence time. As a result, the choice of this parameter depends on the user's specifications.

5 Discussion

Experimental results prove that the chosen control strategy is effective to mitigate long duration disturbance signals, both harmonic and broadband. Even though the convergence time for the broadband signal is higher than that in

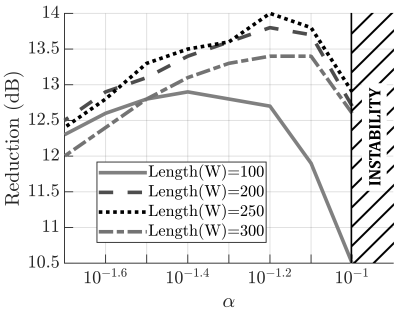

Fig. 12 Global reduction R in function of the adaption gain α, for different filter length.

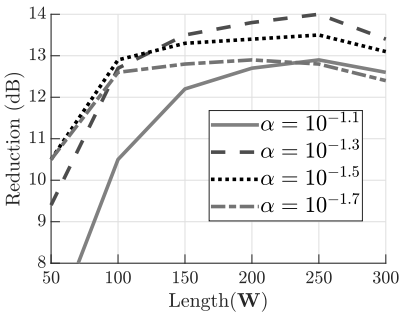

Fig. 13 Global reduction R in function of the filter length, for different adaption gain α.

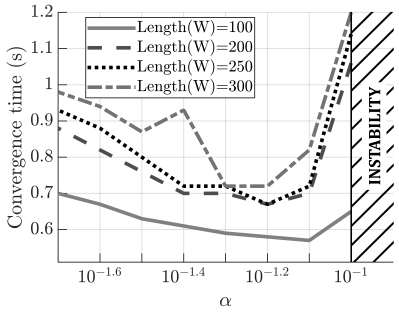

Fig. 14 Global reduction R in function of the adaption gain α, for different filter length.

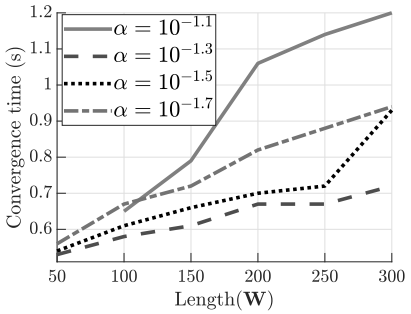

Fig. 15 Global reduction R in function of the filter length, for different adaption gain α.

the harmonic situation, it is nevertheless short enough compared to the typical sources of disturbance in museums, which might last for hours in working construction cases [53, 54], or even be permanent in cases of ventilation systems [16]. In contrast, for shorter duration sources, lasting for less than a few seconds, the convergence time increases and may be too long to preserve cultural heritage objects from degradation. It is known that the FxLMS does not allow fast convergence times, and can even produce instabilities in case of impulse sources. More powerful but more complex adaptive algorithms have recently been developed to overcome this limitation [55].

Global reduction is extremely high for a harmonic source and only passive systems designed to have an anti-resonance at the source frequency can provide such an attenuation. In the case of a broadband noise, reduction drops but still offers significant reduction as vibrations become more than 4 times lower in term of energy. The difference in the performance for harmonic and broadband signals can be explained by the deterministic character of harmonic signals, in contrast with the random character of broadband signals, which are only controllable in certain conditions [56].

Results show that the control system performance drops below 100 Hz. Two improvements can be considered (i) optimising the placement of the transducers, which may enlarge the controlled frequency range, as suggested in [57, 58], (ii) using an actuator with a lower cut-off frequency, but with the disadvantage of a larger size. Other transducers technologies can be experimented, such as piezo electronic [34], but the search for the most appropriate technology for the secondary source is beyond the scope of this article. Finally, a particular attention must be given to the phase of the identification, whose difference with the phase of the real transfer function must not exceed 90° in absolute value for stability reasons [59]. If they do, vibrations are increased in this frequency region, what might lead to a destabilisation of the full control process in the worst cases.

Performances are strongly influenced by the adaptation gain α, which is related to how fast the control filter is able to adapt. It is expected that an increase of α, below an optimal value, tends to reduce the convergence time. However this parameter also affects the global reduction. This is not surprising, as white noise signals are random process whose properties vary when analysed on short windows. If the adaptation gain α is too small, the control filter is not updated fast enough to track the signal variations, and the controller performances decrease. In contrast, if the adaptation gain α exceeds the optimal value shown in Figure 12, the adaptation term added to the coefficients increases, which causes the filter coefficients to oscillate around their optimal values. Moreover increasing the adaptation gain further increases the risk of system instability. This limit can be theoretically calculated [60] but requires to perfectly know the control conditions, in particular the disturbance characteristics, which is not possible in the case of cultural heritage environments. As a result, the adaptation gain should be carefully adjusted in order to offer the best possible reduction, even though it does not necessarily provide the fastest convergence time. To overcome this difficulty, some algorithms propose a dynamic adaptation of α [61], but have not been tested in a cultural heritage context yet.

The other parameter influencing performances is the number of coefficients in the control filter $\mathbf{W}$. When this value decreases, the convergence time τ decreases, but the global reduction R too: indeed, the controller does not have enough coefficients to match the response of the optimal control filter, which represents the filter offering the best performance from a theoretical point of view. When the length of the filter increases, its difference from the best theoretical filter decreases and reaches a minimum. Simultaneously, the global reduction grows until a maximum. Then, increasing this parameter does not have effect anymore on the global reduction. The drawback of increasing the filter length is the rise of the convergence time, which is often encountered with adaptive filter algorithms, both for theoretical [62] and experimental [63] approaches. This phenomenon can be explained by the fact that increasing the number of coefficients increase the number of dimensions of the minimisation problem and extends the calculation time of the global minimum. Furthermore,

the computational complexity, a term related to the number of operations that the algorithm must compute at each time step, increases with the number of coefficients. For real-time applications, the filter length should then be minimised.

Algorithm robustness to amplitude changes is not surprising because the normalised version of the FxLMS has been specifically designed for it. On the other hand, robustness to spectral changes is not guaranteed by the algorithm structure, and instability problems may arise. For each spectral change, each filter coefficient must find a new ideal value starting from a non-null initial condition, what can disrupt the algorithm enough to make it diverge. To recover stability, the adaption gain must be reduced, with the consequences previously mentioned. In order to ensure the robustness of our experimental bench, we suggest to keep the adaptation gain below $10^{-1.1}$.

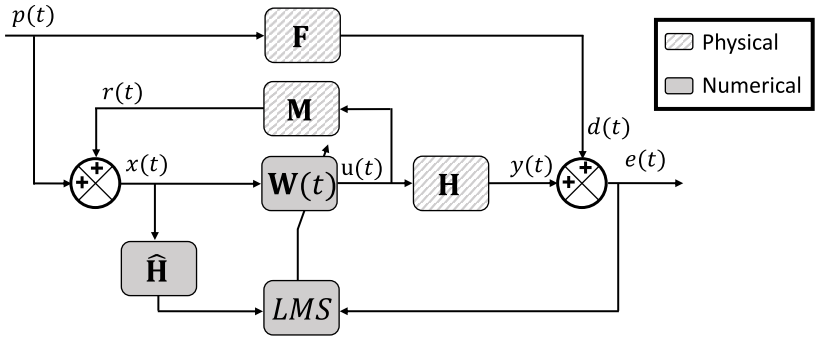

Fig. 16 Block diagram of the controlled system with a FxLMS control algorithm when the reverse path **M** cannot be neglected anymore. The primary and secondary path are respectively represented by the transfer functions **F** and **H**, while $\hat{\mathbf{H}}$ is an estimation of the secondary path. $x(t)$ and $e(t)$ represent respectively the measurements of the reference and error sensors, while $p(t)$ is the contribution of the primary source to the reference sensor. The controller $\mathbf{W}(t)$ is continuously updated by the mean of a LMS procedure using as input the error.

The FxLMS structure assumes that the actuator only contributes to the error measurement. In practice, the vibration can also propagates to the reference sensor and bias the reference signal. As shown in Figure 16, the reference input used in the FxLMS structure $x(t)$ is actually the sum of the contribution of the primary source $p(t)$ and the contribution of the reverse path $r(t)$. This undesirable feedback can decrease the control performances and lead to divergence if the internal closed loop becomes unstable. In our control configuration, preliminary measurements have shown that the contribution, in terms of energy, of the secondary source, is 17.8 dB lower at the reference sensor than at the error sensor (see Figure 17), and 10.2 dB lower in the frequency region of the broadband disturbance (70-400 Hz). This is probably due to the mechanical properties of the shelf and to the relatively large distance between the actuator and the reference sensor in our experimental protocol. Consequently, it allows us to neglect the contribution of the

actuator to the reference signal without dramatic consequences. In other situations, where the reference sensor must be located next to the actuator, this bias cannot be ignored anymore, and algorithms have to compensate for this internal loop. These algorithms include the model of the reverse path in their controller in order to guarantee the stability of the feedback loop [64].

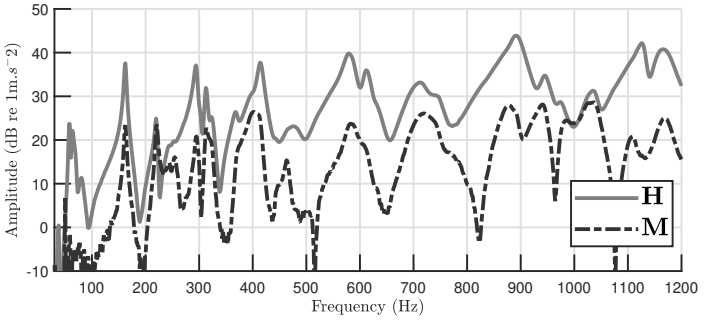

Fig. 17 Frequency response of the secondary path **H** and of the reverse path **M**.

5.1 Conclusion

This work shows that an active control strategy can be successfully applied to vibrations encountered by cultural heritage objects, with consideration for both practical and physical requirements. The choice of the control strategy has been performed considering a list of criterions expressed by the cultural heritage community, the most important being non-intrusion and reversibility, with strong adaptability and practicality. Our system is capable of attenuating broadband disturbances by 14 dB, and is robust to amplitude and frequency content source variations. Compared to common passive solutions, the superiority of this technique lies in its versatility and its ability to mitigate frequencies vibration in a given frequency range. Finally, a parametric study has shown that the greater error attenuation and the fastest control cannot be achieved simultaneously, so the choice of the adaptation gain and the control filter length must result from a compromise.

Results are promising enough to look further into this strategy and future works will focus on two complementary aspects: the improvement of the control effectiveness and the development of an embedded control system. The first one mainly concerns the improvement of algorithm structure, in notably the dynamic adjustment of the adaptation gain and the consideration of the reverse path between the actuator and the reference sensor. To address these questions, more recent algorithms can be considered [64]. To enhance the control performances, other possibility include an optimisation of the transducers position.

The second improvement concerns the design of a transportable and ergonomic device, which requires the consideration of both technical and practical aspects for the choice of the hardware. The controller used in this study is large and expensive, and is therefore not appropriated for a use in cultural heritage context. To replace this device, a micro-controller – an electronic card with an embedded micro-processor – whose properties are chosen to respect practical considerations can be developed. Finding the appropriate actuator seems to be a more difficult challenge. A trade-off must be found between the cut-off frequency, as low as possible, and the size of the component, discrete enough not to interfere with the museography. The solution may also lie in the use of alternative actuator technologies. All these considerations aim to develop an embedded control system with augmented performances, and to perform *in situ* demonstrations within the cultural heritage community.

Acknowledgments. I am personally grateful to the staff of the following museums, that helped me to conduct *in situ* measurements and provide me with materials to build the test bench: Musée de la Musique, Musée du Louvre, Musée du Quai Branly/Jacques Chirac, Musée des Arts Décoratifs and Musée de l'Homme.

Statements and Declarations

This research was supported by Paris Seine Graduate School of Humanities, Creation, Heritage, Investissements d'Avenir ANR-17-EURE-0021-Foundation for Cultural Heritage Science.

The datasets generated during and/or analysed during the current study are available from the corresponding author on reasonable request.

References

[1] Schijve, J.: Fatigue of structures and materials in the 20th century and the state of the art. International Journal of Fatigue **25**(8), 679–702 (2003). https://doi.org/10.1016/S0142-1123(03)00051-3

[2] Mecklenburg, M.F.: Art in Transit: Studies in the Transport of Paintings vol. 1. National Gallery of Art, 'Washington, DC' (1991)

[3] Lasyk, L., Lukomski, M., Bratasz, L., Kozlowski, R.: Vibration as a hazard during the transportation of canvas paintings. Studies in Conservation **53** (2008). https://doi.org/10.1179/sic.2008.53.Supplement-1.64

[4] Bäschlin, N., Läuchli, M., Fankhauser, T., Hoess, A., Palmbach, C.: Backing Boards and Glazing on Paintings: Their Damping Capacity in Relation to Shock Impact and Vibration. ICOM-CC 16th Triennial Conference, Lisbon, Portugal (2011)

[5] Läuchli, M., Bäschlin, N., Hoess, A., Fankhauser, T., Palmbach, C., Ryser, M.: Packing systems for paintings: Damping capacity in relation to transport-induced shock and vibration. ICOM-CC 17th Triennial Conference (2014)

[6] Fatuzzo, G., Sequenzia, G., Oliveri, S., Barbagallo, R., Calì, M.: An integrated approach to customize the packaging of heritage Artefacts, pp. 167–175 (2017). https://doi.org/10.1007/978-3-319-45781-9_18

[7] William, W.: Backing Boards and Glazing on Paintings: Their Damping Capacity in Relation to Shock Impact and Vibration. ICOM-CC 16th Triennial Conference, Lisbon, Portugal (2011)

[8] Smyth, A., Serotta, A.: Managing construction-induced vibration in the museum environment. Objects Specialty Group Postprints **21** (2014)

[9] Wei, W., Watts, S., Seddon, T., Crombie, D.: Protecting museum collections from vibrations due to construction: Vibration statistics, limits, flexibility and cooperation. Studies in Conservation **63**(sup1), 293–300 (2018). https://doi.org/10.1080/00393630.2018.1504438

[10] Higgitt, C., Harrison, L., Galikowski, T., Pau, M., Henson, P.: Protecting the national gallery's paintings collection from the impact of vibration during building work. Studies in Conservation **65**(sup1), 148–153 (2020). https://doi.org/10.1080/00393630.2020.1754058

[11] Lithgow, R., Whittaker, S., Bower, T., Corda, K., Woolley, E., Higgitt, C., Vlachou-Mogire, C., Babington, C.: Vibration monitoring of daniel maclise's wall painting trafalgar. Studies in Conservation **65**(sup1), 180–186 (2020). https://doi.org/10.1080/00393630.2020.1753359

[12] Norén-Cosgriff, K., Ellingsen, S., Resvoll, R., Hov, S.: The new museum of the viking age – assessment of vibration from groundworks to avoid damage to artefacts. Applied Acoustics **196**, 108862 (2022). https://doi.org/10.1016/j.apacoust.2022.108862

[13] Warren, C.H.E.: Recent sonic-bang studies in the united kingdom. The Journal of the Acoustical Society of America **51**(2C), 783–789 (1972). https://doi.org/10.1121/1.1912910

[14] Commins, D.E., A., G., Sirieys, J.P., Fornol, A.: Case-study of Railway Vibrations in Buildings: the Musée d'Orsay. InterNoise, Beijing, China (1987)

[15] Cigada, A., Sabbioni, E., Siami, A., Zappa, E.: Modeling and testing of the anti-vibration base for michelangelo's pietà rondanini. In: Di Miao, D., Tarazaga, P., Castellini, P. (eds.) Special Topics in Structural Dynamics,

Volume 6, pp. 11–21. Springer, Cham (2016)

[16] Cigada, A., Zappa, E., Paganoni, S., Giani, E.: Protecting pietà rondanini against environmental vibrations with structural restoration works. International Journal of Architectural Heritage, 1–16 (2021). https://doi.org/10.1080/15583058.2021.1959674

[17] Costanzo, A., Falcone, S., Piana, C.L., Lapenta, V., Musacchio, M., Sgamellotti, A., Buongiorno, M.F.: Traffic-induced vibrations on cultural heritage in urban area: the case of villa farnesina in rome. Journal of Physics: Conference Series **2204**(1) (2022). https://doi.org/10.1088/1742-6596/2204/1/012043

[18] Lavatelli, A., Zappa, E., Cigada, A., Canali, F.: Monitoring of Environmental and Sound-Induced Vibrations on Artistic Stained Glasses, pp. 399–407 (2020). https://doi.org/10.1007/978-3-030-12676-6_39

[19] Gregorini, A., Paganoni, S., Zappa, E., Cigada, A., Canali, F.: Effects of environmental vibration on ancient stained-glass windows. Journal of Cultural Heritage **56**, 65–74 (2022). https://doi.org/10.1016/j.culher.2022.06.002

[20] Johnson, A., El Batanouny, M.: The effects of vibrations from human traffic and construction on museum collection. Papyrus, the magazine of the International Association of Museum Facility Administators **20**, 4–9 (2019)

[21] Koga, D., Morasset, E., Pepi, R., Woodham, D.: Protecting stained-glass windows from vibrations caused by construction operations. APT Bulletin: The Journal of Preservation Technology **51**(4), 6–12 (2020)

[22] Kracht, K., Kletschkowski, T.: From art to engineering: A technical review on the problem of vibrating canvas part i: Excitation and efforts of vibration reduction. Facta Universitatis. Series: Mechanical Engineering **15**, 163–182 (2017). https://doi.org/10.22190/FUME161010009K

[23] Zini, G., Betti, M., Bartoli, G.: Experimental analysis of the traffic-induced-vibration on an ancient lodge. Structural Control and Health Monitoring **29** (2021). https://doi.org/10.1002/stc.2900

[24] Génevaux, J.-M.: Les courbures locales, limites en fatigue d'un tableau soumis à des vibrations : l'usage des protections arrière. Conservation-restauration des biens culturels (CRBC) **25**, 37–44 (2007)

[25] Génevaux, J.-M., Hamard, G., Lamarins, V., Pringent, T.: Efficacité vibratoire d'une protection arrière rigide de tableau : expérience et modèle. In: 19 Ième Congrès Français de Mécanique, marseille, France, p.

481 (2009)

[26] Génevaux, J.-M., Le Dantec, B.: Optimized anti-vibratory system for stretched canvas artwork hanging in a museum. Journal of Cultural Heritage **15**(4), 382–390 (2014). https://doi.org/10.1016/j.culher.2013.08.001

[27] Santos, F., Fraternali, F.: Novel magnetic levitation systems for the vibration control of lightweight structures and artworks. Structural Control and Health Monitoring **29** (2022). https://doi.org/10.1002/stc.2973

[28] Kuo, S.M.: Adaptive active noise control systems: algorithms and digital signal processing (DSP) implementations. In: Papamichalis, P., Kerwin, R.D. (eds.) Digital Signal Processing Technology: A Critical Review, vol. 10279. SPIE, Orlando (1995). https://doi.org/10.1117/12.204209. International Society for Optics and Photonics

[29] Preumont, A.: Collocated versus Non-collocated Control, pp. 117–130. Springer, Dordrecht (2018)

[30] Coanda: Procédé de protection contre les bruits. (1930)

[31] Olson, H.F., May, E.G.: Electronic sound absorber. The Journal of the Acoustical Society of America **25**(6), 1130–1136 (1953)

[32] Yao, G., Yap, F.F., Chen, G., Li, W., Yeo, S.: Mr damper and its application for semi-active control of vehicle suspension system. Mechatronics **12**, 963–973 (2002). https://doi.org/10.1016/S0957-4158(01)00032-0

[33] Samarasinghe, P.N., Zhang, W., Abhayapala, T.D.: Recent advances in active noise control inside automobile cabins: Toward quieter cars. IEEE Signal Processing Magazine **33**(6), 61–73 (2016). https://doi.org/10.1109/MSP.2016.2601942

[34] Yong, C., Zimcik, D., Wickramasinghe, V., Nitzsche, F.: Development of the smart spring for active vibration control of helicopter blades. Journal of Intelligent Material Systems and Structures **15** (2004)

[35] Şahin, M., Karadal, F., Yaman, Y., Kircali, O., Nalbantoglu, V., Ulker, D., Caliskan, T.: Smart structures and their applications on active vibration control: Studies in the department of aerospace engineering, metu. Journal of Electroceramics **20**, 167–174 (2008)

[36] Chang, C.-M., Spencer Jr, B.F.: Active base isolation of buildings subjected to seismic excitations. Earthquake Engineering & Structural Dynamics **39**(13), 1493–1512 (2010). https://doi.org/10.1002/eqe.1040

[37] Venanzi, I., Ierimonti, L., Materazzi, A.: Active base isolation of museum artifacts under seismic excitation. Journal of Earthquake Engineering **24** (2018). https://doi.org/10.1080/13632469.2018.1453410

[38] Thickett, D.: Vibration damage levels for museum objects. In: ICOM Committee for Conservation 13th Triennial Meeting, Rio de Janeiro (2002)

[39] Eriksson, L., Allie, M., Greiner, R.: The selection and application of an iir adaptive filter for use in active sound attenuation. IEEE Transactions on Acoustics, Speech, and Signal Processing **35**(4), 433–437 (1987). https://doi.org/10.1109/TASSP.1987.1165165

[40] Poole, L., Warnaka, G., Cutter, R.: The implementation of digital filters using a modified widrow-hoff algorithm for the adaptive cancellation of acoustic noise. In: ICASSP '84. IEEE International Conference on Acoustics, Speech, and Signal Processing, vol. 9, pp. 215–218 (1984). https://doi.org/10.1109/ICASSP.1984.1172532

[41] Nelson, P.A., Elliott, S.J.: Active Control of Sound vol. vol. 3. Elsevier Science, ??? (1992)

[42] Akhtar, M., Mitsuhashi, W.: Variable step-size based online acoustic feedback neutralization in single-channel active noise control systems. European Signal Processing Conference (2010)

[43] Ljung, L., Söderström, T.: Theory and Practice of Recursive Identification. The MIT Press Series in Signal Processing, Optimization, and Control, vol. 4 (1983)

[44] Jacobson, C.A., Johnson, C.R., McCormick, D.C., Sethares, W.A.: Stability of active noise control algorithms. IEEE Signal Processing Letters **8**(3), 74–76 (2001). https://doi.org/10.1109/97.905944

[45] Landau, I.D., Alma, M., Airimitoaie, T.-B.: Adaptive feedforward compensation algorithms for active vibration control with mechanical coupling. Automatica **47**(10), 2185–2196 (2011). https://doi.org/10.1016/j.automatica.2011.08.015

[46] Landau, I.D., Airimiţoaie, T.-B., Alma, M.: A youla–kucera parametrized adaptive feedforward compensator for active vibration control with mechanical coupling. Automatica **48**(9), 2152–2158 (2012). https://doi.org/10.1016/j.automatica.2012.05.066

[47] Bershad, N.: Analysis of the normalized lms algorithm with gaussian inputs. IEEE Transactions on Acoustics, Speech, and Signal Processing **34**(4), 793–806 (1986). https://doi.org/10.1109/TASSP.1986.1164914

[48] Landau, I.D., Zito, G.: Digital Control Systems: Design, Identification and Implementations, pp. 201–279. Springer, London (2005)

[49] Duong, H.N., Landau, I.D.: An iv based criterion for model order selection. Automatica **32**(6), 909–914 (1996). https://doi.org/10.1016/0005-1098(96)00020-9

[50] Huang, B., Xiao, Y., Sun, J., Wei, G.: A variable step-size fxlms algorithm for narrowband active noise control. IEEE Transactions on Audio, Speech, and Language Processing **21**(2), 301–312 (2013). https://doi.org/10.1109/TASL.2012.2223673

[51] Burgess, J.C.: Active adaptive sound control in a duct: A computer simulation. The Journal of the Acoustical Society of America **70**(3), 715–726 (1981). https://doi.org/10.1121/1.386908

[52] Elliott, S., Stothers, I., Nelson, P.: A multiple error lms algorithm and its application to the active control of sound and vibration. IEEE Transactions on Acoustics, Speech, and Signal Processing **35**(10), 1423–1434 (1987). https://doi.org/10.1109/TASSP.1987.1165044

[53] Johnson, A.P., Hannen, W.: Vibration limits for historic buildings and art collections, pp. 66–74 (2015)

[54] Smyth, A., Brewick, P., Greenbaum, Y., Chatzis, M., Serotta, A., Stünkel, I.: Vibration mitigation and monitoring: A case study of construction in a museum. Journal of the American Institute for Conservation **55**, 32–55 (2016)

[55] Sun, X., Kuo, S.M., Meng, G.: Adaptive algorithm for active control of impulsive noise. Journal of Sound and Vibration **291**(1), 516–522 (2006). https://doi.org/10.1016/j.jsv.2005.06.011

[56] Hong, J., Bernstein, D.S.: Bode integral constraints, collocation, and spillover in active noise and vibration control. IEEE Trans. Control. Syst. Technol. **6**, 111–120 (1998). https://doi.org/10.1109/87.654881

[57] Jemai, B., Ichchou, M.N., Jezequel, L., Noe, M.: An assembled plate active control damping set-up: optimization and control. Journal of Sound and Vibration **225**(2), 327–343 (1999). https://doi.org/10.1006/jsvi.1999.2250

[58] Wrona, S., Pawełczyk, M.: Controllability-oriented placement of actuators for active noise-vibration control of rectangular plates using a memetic algorithm. Archives of Acoustics **38**(4), 529–536 (2013). https://doi.org/10.2478/aoa-2013-0062

[59] Wang, A.K., Ren, W.: Convergence analysis of the multi-variable filtered-x lms algorithm with application to active noise control. IEEE Transactions on Signal Processing **47**(4), 1166–1169 (1999). https://doi.org/10.1109/78.752618

[60] Vicente, L., Masgrau: Novel fxlms convergence condition with deterministic reference. IEEE Transactions on Signal Processing **54**(10), 3768–3774 (2006). https://doi.org/10.1109/TSP.2006.880205

[61] Landau, I.D., Airimitoaie, T.-B.: Does a general structure exist for adaptation/learning algorithms? In: CDC 2022 - 61st IEEE Conference on Decision and Control, Cancun, Mexico (2022)

[62] Widrow, B., Sterans, S.: Adaptive Signal Processing. Prentice Hall, Englewood Cliffs (1985)

[63] Schüldt, C., Lindstrom, F., Li, H., Claesson, I.: Adaptive filter length selection for acoustic echo cancellation. Signal Process. **89**(6), 1185–1194 (2009). https://doi.org/10.1016/j.sigpro.2008.12.023

[64] Airimitoaie, T.-B., Landau, I.D., Melendez, R., Dugard, L.: Algorithms for adaptive feedforward noise attenuation—a unified approach and experimental evaluation. IEEE Transactions on Control Systems Technology **29**(5), 1850–1862 (2021). https://doi.org/10.1109/TCST.2020.3023276